MR-Guided Delivery of AAV2-BDNF into the Entorhinal Cortex of Non-Human Primates

Alan H. Nagahara[1], **Bayard R. Wilson**[1], **Iryna Ivasyk**[1], **Imre Kovacs**[1], **Saytam Rawalji**[1], **John R. Bringas**[2], **Phillip J. Pivirotto**[2], **Waldy San Sebastian**[2], **Lluis Samaranch**[2], **Krystof S. Bankiewicz**[2,*], and **Mark H. Tuszynski**[1,3,*]

[1]Department of Neurosciences, University of California – San Diego, La Jolla, California 92093, USA

[2]Department of Neurological Surgery, University of California – San Francisco, San Francisco, California 94103

[3]Veterans Affairs Medical Center, San Diego, California 92161, USA

Abstract

Brain-derived neurotrophic factor (BDNF) gene delivery to the entorhinal cortex is a candidate for treatment of Alzheimer's disease (AD) to reduce neurodegeneration that is associated with memory loss. Accurate targeting of the entorhinal cortex in AD is complex due to the deep and atrophic state of this brain region. Using MRI-guided methods with convection-enhanced delivery, we were able to accurately and consistently target AAV2-BDNF delivery to the entorhinal cortex of non-human primates. $86 \pm 3\%$ of transduced cells in the targeted regions co-localized with the neuronal marker NeuN. The volume of AAV2-BDNF (3×10^8 vg/µl) infusion linearly correlated with the number of BDNF labeled cells and the volume (mm^3) of BDNF immunoreactivity in the entorhinal cortex. BDNF is normally trafficked to the hippocampus from the entorhinal cortex; in these experiments, we also found that BDNF immunoreactivity was elevated in the hippocampus following therapeutic BDNF vector delivery to the entorhinal cortex, achieving growth factor distribution through key memory circuits. These findings indicate that MRI-guided infusion of AAV2-BDNF to the entorhinal cortex of the non-human primate results in safe and accurate targeting and distribution of BDNF to both the entorhinal cortex and the hippocampus. These methods are adaptable to human clinical trials.

INTRODUCTION

Alzheimer's disease (AD) is the most common neurodegenerative disorder, and lacks effective disease-modifying therapies. The entorhinal cortex is typically the first brain region affected in AD[1–5], and neuronal degeneration in the entorhinal cortex is associated with what is often the first and cardinal symptom of AD, short-term memory loss[6, 7]. Thus,

*To whom correspondence should be addressed: Krystof.Bankiewicz@ucsf.edu or mtuszynski@ucsd.edu, Telephone: 858-534-8857.

Conflict of Interest Statement: There are no competing financial interests.

therapeutic strategies to slow entorhinal/hippocampal neuronal degeneration could be of substantial value in the treatment of AD.

Brain-derived neurotrophic factor (BDNF) is the most abundant neurotrophic factor in the adult brain, and its levels decline in the entorhinal cortex in AD[8–10]. Previous studies indicate that therapeutic BDNF delivery to the entorhinal cortex of amyloid mutant mice, aged and lesioned rats, as well as aged and lesioned non-human primates, reduces neuronal death, improves synaptic markers, improves molecular signaling and improves hippocampal-dependent learning and memory [11, 12]. Accordingly, BDNF is a candidate for translational human clinical trials[8].

Central nervous system growth factors are medium sized, moderately charged proteins that do not cross the blood brain barrier[13]. Hence, they must be administered into the CNS directly to access degenerating neuronal populations[8]. However, when growth factors broadly spread through the CNS, they elicit intolerable adverse effects including weight loss, sensory disturbances and Schwann cell migration into the CNS[8]. Thus, their testing in clinical trials requires delivery methods that achieve both central and *restricted* delivery solely to regions of degenerating neurons. Gene delivery is a potential means of accomplishing this goal. We recently reported that gene delivery of another growth factor to the basal forebrain region of AD patients, nerve growth factor (NGF), was safe and well tolerated, and elicited classic "trophic" responses from degenerating cholinergic neurons[14]. Yet a 49 patient, double blind, sham surgery-controlled Phase 2 trial did not show efficacy in reducing cognitive decline (https://clinicaltrials.gov/ct2/show/NCT00876863). However, gene delivery was off-target in at least half of the intended sites in these patients based on examination of several brains, despite the use of state-of-the-art clinical stereotaxic methods and planning software (unpublished observations). This highlights the need to utilize more accurate methods for targeting and distributing growth factors in human clinical trials. Image-guided vector delivery is a potential method for achieving this important goal.

The entorhinal cortex is located on the ventromedial surface of the temporal lobe. It is an elongate structure 30 mm in antero-posterior length, 9–18 mm in width (along the cortical surface), and 3 mm thick[15]. Accordingly, accurately targeting this structure, which becomes atrophic in AD[16, 17], is a challenge when using conventional stereotaxic approaches.

Recently we developed methods to enhance vector targeting and distribution in intracranial regions using MRI-guided infusions together with co-infusions of the safe MR contrast agent gadoteridol [18, 19,20, 21]. Subjects undergo MRI scans during brain infusions, demonstrating real-time vector infusion and distribution. Combining this approach with convection-enhanced infusion procedures can further optimize vector distribution in the brain [22]. This approach has been implemented in clinical trials for brain tumors[23], growth factor and enzymatic gene therapy for Parkinson's disease[24], and gene replacement in aromatic acid decarboxylase (AADC) deficient children[25].

We adapted these previously described methods in an effort to accurately target the entorhinal cortex in non-human primates as part of a translational program of AAV2-BDNF gene therapy for AD. We now report improved targeting and distribution of AAV2-BDNF in

the non-human primate brain using MRI-guided convection-enhanced vector delivery with co-infusion of gadoteridol. The distribution of gadoteridol on initial MRI scan correlated highly with actual vector distribution by BDNF immunolabeling of brains. BDNF protein is effectively anterogradely distributed to the hippocampus after entorhinal cortex delivery. Accordingly, these findings support the use of this improved method for therapeutic growth factor gene delivery in upcoming clinical trials of AAV2-BDNF gene delivery in AD.

RESULTS

A total of 18 adult monkeys of both genders underwent infusion of AAV2-BDNF into the entorhinal cortex (detailed in Methods), including five cynomologus macaques and 13 rhesus macaques. An MR-compatible stereotaxic frame was attached to the skull that guided passage of an MR-compatible infusion needle fabricated from ceramic[26]. Deeply sedated subjects were placed in a 3 Tesla General Electric MR scanner, and needle targeting to the medial entorhinal cortex was assisted by MR guidance (see Methods). The medial entorhinal cortex is located in the most ventral and medial aspect of the frontal lobe (Figs. 1–3). Upon needle positioning, subjects received infusions of AAV2-BDNF (0.3×10^{12} vg/ml) mixed with the MR-dense substance, gadoteridol 2 mM. Subjects received 1–3 infusions per side in volumes ranging from 15–130 μl/site; a range of volumes and sites was used because we continued infusions until the targeted brain region was *filled*; for example, if some vector was initially infused into a subcortical white matter region instead of the intended target, the needle was re-positioned and additional vector was infused. There was no effort to infuse a pre-planned *volume* of vector; instead, we continued infusions until the target brain region received vector, regardless of total volume infused. After pre-planned survival periods of 1–6 months, brains were examined for accuracy of BDNF targeting to the entorhinal cortex and cell type infected with AAV2. Vector spread as measured by gadoteridol diffusion was compared to distribution of the intended gene product by tissue labeling using BDNF immunoabeling. We then correlated the total volume of vector infused per site to volume of brain transduced by BDNF immunolabeling (see Methods).

Targeting the Entorhinal Cortex

In the monkey, the entorhinal cortex is located, as in the human, in the medial temporal lobe (Fig. 1). This brain region receives inputs from broad regions of the cortex, and in turn directly projects to the dentate gyrus of the hippocampus[27–29]. Outputs from the hippocampus then return to the entorhinal cortex, which sends projections to other cortical regions that are sites of long term memory storage, as well as the parahippocampus gyrus and perihinal cortex[30, 31]. This neural circuitry is essential for learning and memory[31–33]. In the rhesus monkey, the entorhinal cortex is about 15mm in total rostral-to-caudal extent, 5–9 mm wide, and 2–3mm in depth from the cortical surface, with an estimated volume of 255 mm[34]. Grossly, this brain region is located on the ventral most aspect of the medial temporal lobe, and its most ventrolateral component is demarcated by the rhinal fissure (Fig. 2). It's more dorsal extent reaches the amygdala (rostral half) and subicular region (caudal half). Both the rhinal fissue and subicular region can be recognized on MRI scans (Fig. 2). The midpoint of the antero-poster range of the entorhinal cortex (e.g., coordinate 0.75 cm relative to either end of the 1.5 cm length of the entorhinal cortex) is recognizable on MRI scans as

the point at which the hippocampus first becomes evident on coronal brain sections. The cortical surface is also visible on MRI scans, and these infusions aim to be centered 1mm below this surface. Thus, for all three dimensions of the entorhinal cortex, there are fiducial markings that are recognizable on MRI scans: 1) in the antero-posterior plane, the first appearance of the hippocampus on coronal brain sections (1mm thick slices); 2) in the medio-lateral plane, the shape of the amygdala/subiculum (dorsal) and the rhinal fissure (lateral); and 3) in the ventro-medial plane, the cortical surface (Fig. 2). We used these MRI landmarks to target vector infusions. Animals received from one to three vector infusions per side of the brain. The present study focused on the question of whether we are able to use MRI guidance with gadoteridol infusion to reliably infuse AAV2-BDNF into this small brain region.

MRI-Guided Infusions Enable Precise, Accurate Gene Delivery to the Entorhinal Cortex

The injection needle could be readily visualized on MRI scans of the brain, as expected (Fig. 3A). This allowed confirmation of the accuracy of stereotaxic targeting. Typically, 1–2 adjustments of needle depth were required to accurately infuse the brain region of interest, but medio-lateral and rostral-caudal trajectories were in nearly all cases accurate without requiring needle withdrawal and repositioning.

With positioning of the infusion needle in the entorhinal cortex at a depth of 1mm from the cortical surface, infusion of the AAV2-BDNF / gadoteridol solution resulted in vector spread in cortical layers I–II over a rostral-to-caudal distance of 5–8mm (green arrows in Fig. 3E–F). Occasionally, the tip of the infusion needle appeared to exit the ventral surface of the brain with resulting gadoteridol spread in the subarachnoid space; in these cases, the MRI tracer signal rapidly dissipated (within 10 min). When infusions were located intraparenchymally, gadoteridol signal was persistently detectable over at least 30 min on MRI.

Correlation of Gadoteridol Diffusion with BDNF Transduction

Anatomical examination of infused brains using BDNF immunolabeling demonstrated that vector spread assessed by gadoteridol on MRI scans during infusions closely matched in vivo BDNF gene expression (Fig. 3). Thus, gadoteridol spread at the time of vector infusion accurately reflected vector spread on histological examination.

AAV2- Primarily Infects Neurons of the Entorhinal Cortex

Quantification of BDNF or GFP co-labeling with the neuronal marker NeuN indicated that AAV2 primarily infected neurons in the entorhinal cortex. Among the subjects that received AAV2-GFP, $88.2 \pm 3.8\%$ of cells expressing GFP were neurons, as assessed by double labeling with NeuN. Among BDNF labeled cells, $85.9 \pm 3.5\%$ were co-labeled with NeuN (Fig. 4). As expected, cell transduction in white matter regions such as the angular bundle was low due to the absence of neurons in these regions.

Entorhinal Cortex BDNF Expression Correlates with Vector Infusion Volume

The volume of vector distribution of BDNF and GFP in the entorhinal cortex was measured in BDNF- and GFP-immunolabeled sections (Fig. 5). The volume of infused vector

correlated significantly with the volume of transduced entorhinal cortex (r(24)=0.73, p<0.0001; Fig. 5D). Overall, across all animals with accurate vector targeting to the entorhinal cortex, the proportionate volume of transduced entorhinal cortex was 59.9 ± 6.7%. The total volume of vector infused among these subjects ranged from 15–184 μl per entorhinal cortex, spread over 1–3 infusions sites. Subjects with the greatest volume of BDNF expression in the entorhinal cortex generally received the highest number of infusions, reliably exhibiting >50% transduction of the entorhinal cortex with BDNF. A significant correlation also existed between the volume of the infused vector and the number of neurons expressing BDNF in the entorhinal cortex (r(22)=0.82, p<0.0001; Fig 5E). While the total volume of vector infusion was an important consideration in maximizing the volume of entorhinal cortex transduction, accurate positioning of the infusion needle to a depth of approximately 1mm from the ventral surface of the entorhinal cortex most consistently assured distribution within the target region.

BDNF Trafficking to Hippocampus

AAV2-BDNF vector Infusion into the entorhinal cortex has previously been reported to result in anterograde trafficking of BDNF protein into the hippocampus[11, 12]. We also found this to be the case in the present study (Fig 6A–D). Even relatively small volumes of BDNF transduction of the entorhinal cortex (e.g., 15μl), when accurately targeted, resulted in widespread increases in BDNF labeling in the hippocampal dentate gyrus.

DISCUSSION

BDNF gene delivery to the entorhinal cortex offers the potential to slow the degeneration and death, and stimulate the function, of cortical neurons that are affected in AD[8, 11, 12]. Findings of the present study indicate that the ability to accurately target this deep brain structure is substantially improved using real-time MRI targeting and co-infusion of gadoteridol. In previous experiments we targeted vector injections into the non-human primate entorhinal cortex using stereotaxic coordinates only, without MRI guidance; these efforts resulted in accurate vector delivery into the entorhinal cortex in less than 50% of sites (data now shown). Injections were often off-target, located more frequently in the angular gyrus (subcortical white matter) and resulted in vector loss through white matter tracks with little transduction of gray matter. Using methods described in this study, we accurately target the entorhinal cortex in more than 95% of monkeys, and can distribute vector over at least 50% of the volume of the target. These methods are safe and well-tolerated, and to date there have been no peri-operative complications after infusing a total of 18 monkeys.

Consistent with infusions of vector into other brain regions[21, 25, 35, 36], the volume of entorhinal cortex transduction with AAV2-BDNF correlated with the volume of vector infusion when infusions were accurately targeted into the entorhinal cortex. However, when the infusion needle tip was located in subcortical white matter, vector rapidly diffused through white matter and did not efficiently transduce the entorhinal cortex. In this small gray matter region, it appears that accuracy of needle placement is the most important consideration in effectively distributing AAV2-BDNF. Without real-time imaging and gadoteridol co-infusion, the entorhinal cortex was not consistently engaged in non-human

primates, and likely would not be in a human clinical trial. Indeed, preliminary observations from our recent experience targeting another small brain region in AD patients with NGF gene delivery, the Nucleus Basalis of Meynert, showed mis-targeting of several injections, despite the fact that the trial used state-of the-art stereotaxic methods and experienced neurosurgeons (clinicaltrials.gov). These observations indicate that the development of more accurate, real-time MRI guided methods for gene delivery to smaller brain targets will be important for advancing future programs to human trials.

An important observation in this study was that BDNF is consistently trafficked into the hippocampus when AAV2-BDNF is accurately delivered to the entorhinal cortex. BDNF transport to the hippocampus could extend the distribution of BDNF in the AD brain, thereby accessing the brain regions that are affected the earliest and most extensively in AD[11, 12]. By the time that AD is first diagnosed in humans, up to 50% of neurons in the entorhinal cortex have already degenerated[7]. Notably, pathology in the AD brain typically spreads from the entorhinal cortex to more distant brain regions; indeed recent findings suggest that spread of toxic protein species from the entorhinal cortex may propagate AD pathology to other brain regions[4, 5, 37, 38]. If this is true, then early reduction or arrest of cell degeneration in the entorhinal cortex and hippocampus could reduce the progression of AD. Targeting the entorhinal cortex and hippocampus with BDNF could therefore extend neuroprotection to broader cortical regions. And as the ability to detect AD risk at pre-symptomatic stages of the disease advances[39, 40], there is potential to begin intervention with BDNF in patients at early time points, before cell loss is extensive.

SUMMARY

MRI guidance with co-infusion of gadoteridol permits accurate delivery of AAV2-BDNF to the non-human primate entorhinal cortex. The establishment of these methods enables potentially more effective clinical translation of this approach in an effort to prevent neuronal loss and stimulate neuronal function in AD.

METHODS

Subjects

Subjects were 5 adult cynomolgus macaques (Macaca fascicularis; 5.9–10.0 kg; 4 males, 1 female; age range 3–14 years) and 13 adult rhesus macaques (Macaca Mulatta; 6.0–18.7 kg; 9 males, 4 females; age range 5–21 years). Animals were housed in a temperature-controlled environment with 12-hour light/dark cycle. All subjects were seronegative for the presences of anti-AAV antibodies with antibody titers of <1:100, using previously described protols[41]. All procedures were carried out in accordance with the Institutional Animal Care and USE Committee at UCSF and UC Davis.

Vector Production and Preparation

AAV2-BDNF vector was produced by UNC Vector Core (University of North Carolina) The vector genome consist of the human BDNF cDNA with a CAG promoter consisting of human cytomegalovirus (CMV) enhancer, chicken β-actin promoter and splice donor, intron, an rabbit β-globin splice acceptor. The vector is similarly designed to AAV2 vector used in

Phase 1 and 2 gene therapy trials[14, 42, 43]. Briefly, vector particles were prepared by transient transfection of plasmid DNA into 293 cells and purified by $CsCl_2$ centrifugation, FPLC and sterile filtration. AAV2-BDNF vector was delivered at a titer of 3×10^{12} vg/ml and aliquotted into 100 μl volumes. For infusions, AAV2-BDNF was infused at a concentration of 3×10^{11} vg/ml. The MR contrast agent Gadoteridol (Prohance, Bracco Diagnostic, Princeton, NJ) was mixed into the vector at a final concentration of 1 mM. A subset of subjects (N=9) also received AAV2-GFP at 0.03×10^{12} vg/ml titer to confirm the spread of the viral vector in the transduction of cells.

Surgical Exposure

After induction of anesthesia, the animal's head was placed in a stereotactic frame and flexed in a prone position. The head was shaved and cleaned using Nolvasan solution and alcohol. A sterile field was created and a midline incision performed through the skin, muscle and fascia by electrocautery (Surgistat Electrosurgery, Valleylab Inc., Boulder, CO). Gentle retraction of fascia and muscle allowed for cranial exposure over cortical entry sites. Small burr-holes were performed according stereotactic coordinates to expose dura over each of the intended infusion sites. The infusion system included *i)* a "ball-joint" style array (Hayes Manufacturing Services Inc., USA) that was secured to the skull by titanium screws over the craniotomies, and *ii)* a custom-designed cannula (Richardson et at 2011). The custom-designed, ceramic, fused silica reflux-resistant cannula (Fiandaca et al, 2008) consist of an 8 to 25-cm ceramic section [1.68 mm outer diameter (OD)] in the main portion of the shaft, and an 18-mm fused silica section that tapers down to 0.7 mm OD. The final 3-mm section is a fine fused silica tip (0.36 mm OD). Briefly, the cannula is connected to a loading line containing the infusate, and flow is regulated with a 1-mL syringe mounted onto a MRI-compatible infusion pump. Target is selected and optimal trajectory is established using neuronavigation software on baseline MRI images of the animal. Then, distance from the target to the top of the guide-stem is determined in silico, and a depth-stop is secured at the insertion distance in the cannula. After optima infusion parameters are determined, cannulas are manually inserted though the guiding stem of the array to the target.

MRI-Guided Infusion Procedure

We used a 3 Tesla Siemens Magnetom Avanto scanner (Siemens Medical Solutions, Erlangen, Germany) with Siemens resident software. Vector infusion procedures were done using three types of scanning protocols that were varied throughout the gene delivery procedure: a T1 protocol to optimize visualization of brain structures for the purpose of needle targeting, and modified T2 protocol to obtain a rapid scan to assess vector spread, and an MP-RAGE protocol to optimize visualization of white matter structure and vector spread (Repetition time: 2110 ms; echo time: 3.6 ms; flip angle: 15°; number of excitations: 1 (repeated three times); matrix: 240×240; field of view: $240 \times 240 \times 240$).

Animals were sedated with an intramuscular injection of ketamine (10 mg/kg IM) and medetomidine (0.015 mg/kg IM), intubated, and a venous line established with a 22–24-gauge catheter positioned in the cephalic or saphenous vein to deliver isotonic fluids at a rate of 5–10 mL/kg/hr. Isoflurane inhalation anesthesia (Aerrane, Omeda PPD Inc., Liberty, NJ) was delivered at 1–3% to maintain a stable plane of anesthesia. Then, after placement into an

MRI-compatible stereotaxic frame in a supine position, two burr holes were placed for implantation of ball-joint arrays that consist of a base (attached to the skull) and a guide tube array (cylinder with three holes)[44]. The monkeys were then transferred to the MRI scanner suite. The infusion needle consisted of a ceramic silica reflux-resistant cannula with a 1-mm step at the distal end to prevent vector reflux up the cannula (MRI Intervention, Irvine).[25] Then a 36-inch high-pressure intravenous tubing connected the infusion needle to a 1-ml syringe pump (Medfusion 3500 syringe pump, Medfusion, St Paul, MN). Prior to loading into the infusion system, vector was adjusted to a final concentration of 3.0×10^{11} vg/ml. In nine subjects, one-tenth of the vector infusate volume consisted of AAV2-GFP (3×10^{11} vp/ml) and 90% of the vector consisted of AAV2-BDNF (3×10^{11} vg/ml); these monkeys enabled analysis of the type of cells in the brain that were transduced by the virus. In initial subjects, the infusion needle was placed into the skull-based stereotaxic frame and advanced into the brain to a point calculated to be located in the mid-striatum; the accuracy of needle trajectory and depth were then confirmed with a T2 scan. Because none of these mid-trajectory scans required correction of needle trajectory, all subsequent subjects underwent lowering of the infusion needle into the entorhinal cortex itself, stopping at a point calculated on initial MRI scans to be located 1 mm dorsal to the intended target region. Then, a T1, MP-RAGE and T2 weighted set of images were obtained. Based on these images, we then advanced the infusion needle the distance required to reach a point within the entorhinal cortex that was located 1 mm from the ventral brain surface (Fig. 2).

Monkeys received 1 to 3 infusion sites into the entorhinal cortex per side of the brain. For a single infusion per side, the injection was placed approximately at the mid-point of the antero-posterior length of the hippocampus. For entorhinal cortex that received 2–3 infusions, attempts were made to spread vector through the majority of the volume of the entorhinal cortex. For this study, 34 entorhinal cortices were infused with AAV2-BDNF (3×10^{11} vg/mL): 18 received a single infusion site per side of the brain, 9 received two infusions, and 7 receiving three infusions

At the point that infusion needles were going to penetrate the brain, infusions pumps were turned on at a rate of 3 μl/min to maintain positive pressure and prevent needle blockade as the needle was advanced through the brain to the target. Once the final target was confirmed on MRI, infusion rate was adjusted ramping from 1 up to 3 μl/min to achieve vector spread through the entorhinal cortex region located in the 1mm-thick MRI slice containing the infusion needle. Rather than infuse a pre-set volume of *vector*, we continued infusions until the target region of interest (about 5 mm of the rostral-cadual extent of the entorhinal cortex) was covered by gadoteridol. Scans were continuously obtained through the infusion procedure, as previously described[21, 25]. The range of vector volume infused per site was 15 – 160 μl. Vital signs were monitored continuously during surgery.

After completion of infusions, subjects were returned to the surgical suite for removal of the skull-based stereotaxic frame. Then, animals received an intramuscular injection of NSAID (Meloxicam) and buprenorphine (Buprenex) the day after the CED infusion as part of the post-procedural analgesia management. Once the animal returned to its cage, it was evaluated twice daily for 5 days by veterinary staff. Detailed, standardized forms were completed for each animal that included evaluations of the surgical-site integrity, edema,

infection, balance, locomotion, attitude, food intake, and fecal and urine output. No abnormalities or signs of discomfort were reported.

Histology

Subjects were euthanized 1–6 months following MRI-guided infusions. Subjects were anesthetized as described previously using an intravenous overdose of sodium pentobarbital solution (B-euthanasia solution, 390 mg/ml). Death was confirmed by loss of heartbeat, respiration, pupil reflex and/or toe pinch reflex. Then, animals were transcardially perfused with cold 0.9% Phosphate-buffered saline (PBS) followed by 4% paraformaldehyde (PFA). Brains were harvested and placed in a 10% glycerol solution for one night then transferred to 20% glycerol. Histology was performed at UCSD. The brain was sectioned into 3 blocks, with the most caudal block containing the entorhinal cortex and hippocampus. Blocks were frozen in 99% isopentane and stored at −80°C until sectioning. Sectioning was performed on a sliding microtone set at 40 μm thickness and each section was placed in 96-well polyethylene plates containing cryoprotectant. Tissue was stored at −20°C.

Nissl Staining and Immunohistochemistry

A series of 1-in-12 sections were processed for Nissl staining used standard protocols. Another series of 1-in-24 sections were used for light level immunolabeling of BDNF using antigen retrieval method to enhance labeling. Antigen retrieval procedure involved sections in 0.01 M Tris-HCL (pH 9.0, at 80°C) for 50 min and post-fixation in 2% paraformaldehyde: 0.2% para-benzoquinone for 5 min. Sections were incubated in primary rabbit anti-BDNF antibody (Chicago Proteintech; made for Tuszynski laboratory) at 1:2000 dilution for 4 nights at 4°C. Sections were then incubated in secondary antibody (donkey anti-rabbit biotin, Jackson Immunoresearch Laboratory 711-065-152) using the ABC Reagent kit (Vectastain, Vector Laboratories; PK-6100), and were subsequently developed in 3,3′-diamaniobenzidine. Additional series of 1-in-24 sections were also processed for fluorescent labeling using rabbit anti-BDNF antibody (1:1500, Chicago Proteintech), mouse anti-NeuN (1:2000, clone 1B7, Abcam; AB104224), and chicken anti-GFAP (1:500, Aves Lab; Cat# GFAP) for 4 nights and developed with Alexa Fluor secondary antibodies (1:200, Jackson ImmunoResearch Laboratories; Donkey Anti-Rabbit Alexa594 #711-585-152; Donkey Anti-Mouse #715-605-150; Donkey Anti-Chicken Alex 647 #703-605-152) and 1:1000 DAPI (Sigma D9542). Sections were mounted onto gelled slides and coverslip using Fluoromount-G (Southern Biotech).

AAV2-BDNF and AAV2-GFP Targeting of Neurons

Infusion of AAV2-BDNF and AAV2-GFP resulted in increased expression of the construct in cells at the infusion site. To determine the percentage of cells with elevated BDNF or GFP in neurons, sections were tripled labeled for BDNF, GFP, and NeuN. Quantification was performed at individual infusion sites with selected samples taken across all layers of entorhinal cortex, including the angular bundle (white matter adjacent to entorhinal cortex). The percentage of cells co-labeled for BDNF or GFP with the neuronal marker NeuN was calculated.

Distribution of Vector Expression in Entorhinal Cortex

To determine the spread of the vector at entorhinal cortex infusion sites, BDNF immunolabeled cells were mapped using using Stereoinvestigator (Microbrightfield Bioscience). Sections labeled for BDNF at both fluorescence and light levels were used to enhance accuracy. Regions were sampled at section intervals of 1-in-12 to 1-in-48 sections. For each section, the entorhinal cortex was outlined based on anatomical features (e.g., rhinal fissure) and cytoarchitectural structures of the entorhinal cortex as viewed with NeuN labeling or adjacent Nissl stained sections[45]. A total of 25 entorhinal cortex infusion sites were mapped for the distribution of the BDNF immunolabeled cells and over 100,000 individual cells were mapped. The each BDNF cell was marked as neuronal or non-neuronal based on NeuN labeling.

The StereoInvestigator software provides the X-Y location of the cells. Using a protocol developed by A. Nagahara, Excel (Microsoft) templates were used to map the area of elevated BDNF expression. Briefly, using 300-um bins for both y-axis and x-axis (e.g., 0–300, 301–600), the lowest and highest values were used as the border for each bin, and the area of BDNF expression was calculated in each anatomical section. To confirm this analysis, a Matlab program was written (I. Ivasyk) that utilized the BDNF location data to outline and measure the area of BDNF expression in each anatomical section. Based on these analyses, the total volume of BDNF protein expression was calculated by multiplying area per section by the sampling frequency of 1-in-12 sections and the thickness of each section. The estimated number of neurons that were labeled for BDNF cells was also quantified in 1-in-12 sections, with total neuron numbers estimated based on section sampling frequency (1-in-12). The volume of tissue expressing BDNF was correlated to BDNF-expressing cell numbers.

BDNF Elevation in Entorhinal Cortex and Hippocampus

BDNF protein can be trafficked anterogradely through axonal transport from neurons in the entorhinal cortex to the hippocampus[12], providing a potential means of distributing BDNF throughout entorhinal cortex and into hippocampus following gene delivery to the entorhinal cortex[11, 12]. Previously we reported that co-infusion of AAV2-GFP with AAV2-BDNF into the entorhinal cortex of rhesus macaques did not result in anterograde transport of the AAV2-GFP vector itself into the hippocampus[11], indicating that all BDNF protein that is present in the hippocampus results from anterograde transport of the protein, and not the AAV2-BDNF vector. To examine the extent of BDNF distribution into the hippocampus, we quantified regions of BDNF immunoreactivity in the hippocampal dentate gyrus 1-in-24 sections were scanned with a 2× objective lens on a Keyence (BZ-X700) microscope. The outer molecular layer of dentate gyrus was outlined in Adobe Photoshop software. Threshold analysis was used to determine the area with elevated BDNF levels in the entorhinal cortex and hippocampus. The threshold was based on the BDNF immunolabeling in control cortical brain regions (parietal or temporal cortex). The threshold was calculated from control cortical sample (15,000 pixels) and set at three times the standard deviation above the mean value. A standard threshold value was not used due to the variation of BDNF immunolabeling from subject to subject. Images were imported into ImageJ software and the percent of the region above the threshold value was calculated. Similar measures of

fiber density were made in a series of 1-in-48 sections through the full rostral-to-caudal extent of the hippocampus.

Statistical Analyses

Pearson correlational analyses were performed between the volume of AAV2-BDNF infused and the volume of tissue with BDNF labeled neurons or the estimated number of BDNF-labeled neurons (JMP software from SAS). The sample size of the subjects for this study (N=18) was based on a power analysis using a large effect size for correlational analyses (0.50), a power of .85, and the assumption of 90% accuracy of targeting (inclusion criteria). Only Infusion sites that accurately targeted the entorhinal cortex were included for these analyses. Since group differences were not examined, randomization was not used in the present study. The experimenters were blinded for data collection. The Pearson correlational analysis was determined to be the appropriate analyses that meet the basic assumptions of this statistical test. Since there are no group comparisons, variance data are not presented.

Acknowledgments

References

1. Kfoury N, Holmes BB, Jiang H, Holtzman DM, Diamond MI. Trans-cellular propagation of Tau aggregation by fibrillar species. J Biol Chem. 2012; 287(23):19440–51. [PubMed: 22461630]

2. Mirbaha H, Holmes BB, Sanders DW, Bieschke J, Diamond MI. Tau Trimers Are the Minimal Propagation Unit Spontaneously Internalized to Seed Intracellular Aggregation. J Biol Chem. 2015; 290(24):14893–903. [PubMed: 25887395]

3. Braak H, Braak E. Neuropathological stageing of Alzheimer-related changes. Acta Neuropathol (Berl). 1991; 82(4):239–59. [PubMed: 1759558]

4. Su JH, Deng G, Cotman CW. Transneuronal degeneration in the spread of Alzheimer's disease pathology: immunohistochemical evidence for the transmission of tau hyperphosphorylation. Neurobiol Dis. 1997; 4(5):365–75. [PubMed: 9440125]

5. de Calignon A, Polydoro M, Suarez-Calvet M, William C, Adamowicz DH, Kopeikina KJ, et al. Propagation of tau pathology in a model of early Alzheimer's disease. Neuron. 2012; 73(4):685–97. [PubMed: 22365544]

6. Gomez-Isla T, Price JL, McKeel DW, Morris JC, Growdon JH, Hyman BT. Profound loss of layer II entorhinal cortex neurons occurs in very mild Alzheimer's disease. J Neurosci. 1996; 16:4491–4500. [PubMed: 8699259]

7. Kordower JH, Chu Y, Stebbins GT, DeKosky ST, Cochran EJ, Bennett D, et al. Loss and atrophy of layer II entorhinal cortex neurons in elderly people with mild cognitive impairment. Ann Neurol. 2001; 49(2):202–13. [PubMed: 11220740]

8. Nagahara AH, Tuszynski MH. Potential therapeutic uses of BDNF in neurological and psychiatric disorders. Nat Rev Drug Discov. 2011; 10(3):209–19. [PubMed: 21358740]

9. Connor B, Young D, Yan Q, Faull RL, Synek B, Dragunow M. Brain-derived neurotrophic factor is reduced in Alzheimer's disease. Brain Res Mol Brain Res. 1997; 49(1–2):71–81. [PubMed: 9387865]

10. Narisawa-Saito M, Wakabayashi K, Tsuji S, Takahashi H, Nawa H. Regional specificity of alterations in NGF, BDNF and NT-3 levels in Alzheimer's disease. Neuroreport. 1996; 7(18): 2925–8. [PubMed: 9116211]

11. Nagahara AH, Mateling M, Kovacs I, Wang L, Eggert S, Rockenstein E, et al. Early BDNF treatment ameliorates cell loss in the entorhinal cortex of APP transgenic mice. J Neurosci. 2013; 33(39):15596–602. [PubMed: 24068826]

12. Nagahara AH, Merrill DA, Coppola G, Tsukada S, Schroeder BE, Shaked GM, et al. Neuroprotective effects of brain-derived neurotrophic factor in rodent and primate models of Alzheimer's disease. Nat Med. 2009; 15(3):331–7. [PubMed: 19198615]

13. Poduslo JF, Curran GL. Permeability at the blood-brain and blood-nerve barriers of the neurotrophic factors: NGF, CNTF, NT-3, BDNF. Brain Res Mol Brain Res. 1996; 36(2):280–6. [PubMed: 8965648]

14. Tuszynski MH, Yang JH, Barba D, U HS, Bakay RA, Pay MM, et al. Nerve Growth Factor Gene Therapy: Activation of Neuronal Responses in Alzheimer Disease. JAMA Neurol. 2015; 72(10): 1139–47. [PubMed: 26302439]

15. Mai, JK., Paxinos, G. Atlas of the Human Brain. Vol. 2004. Academic Press; 2007.

16. Juottonen K, Laakso MP, Insausti R, Lehtovirta M, Pitkanen A, Partanen K, et al. Volumes of the entorhinal and perirhinal cortices in Alzheimer's disease. Neurobiol Aging. 1998; 19(1):15–22. [PubMed: 9562498]

17. Pennanen C, Kivipelto M, Tuomainen S, Hartikainen P, Hanninen T, Laakso MP, et al. Hippocampus and entorhinal cortex in mild cognitive impairment and early AD. Neurobiol Aging. 2004; 25(3):303–10. [PubMed: 15123335]

18. Saito R, Bringas JR, McKnight TR, Wendland MF, Mamot C, Drummond DC, et al. Distribution of liposomes into brain and rat brain tumor models by convection-enhanced delivery monitored with magnetic resonance imaging. Cancer Res. 2004; 64(7):2572–9. [PubMed: 15059914]

19. Krauze MT, McKnight TR, Yamashita Y, Bringas J, Noble CO, Saito R, et al. Real-time visualization and characterization of liposomal delivery into the monkey brain by magnetic resonance imaging. Brain Res Brain Res Protoc. 2005; 16(1–3):20–6. [PubMed: 16181805]

20. Fiandaca MS, Varenika V, Eberling J, McKnight T, Bringas J, Pivirotto P, et al. Real-time MR imaging of adeno-associated viral vector delivery to the primate brain. Neuroimage. 2009; 47(Suppl 2):T27–35. [PubMed: 19095069]

21. Su X, Kells AP, Aguilar Salegio EA, Richardson RM, Hadaczek P, Beyer J, et al. Real-time MR imaging with Gadoteridol predicts distribution of transgenes after convection-enhanced delivery of AAV2 vectors. Mol Ther. 2010; 18(8):1490–5. [PubMed: 20551915]

22. Krauze MT, Forsayeth J, Yin D, Bankiewicz KS. Convection-enhanced delivery of liposomes to primate brain. Methods Enzymol. 2009; 465:349–62. [PubMed: 19913176]

23. Jahangiri A, Chin A, Flanigan PM, Chen R, Bankiewicz K, Aghi MK. Convection Enhanced Delivery in Glioblastoma: A Review of Preclinical and Clinical Studies. J Neurosurg. In press.

24. Richardson RM, Kells AP, Rosenbluth KH, Salegio EA, Fiandaca MS, Larson PS, et al. Interventional MRI-guided putaminal delivery of AAV2-GDNF for a planned clinical trial in Parkinson's disease. Mol Ther. 2011; 19(6):1048–57. [PubMed: 21343917]

25. San Sebastian W, Kells AP, Bringas J, Samaranch L, Hadaczek P, Ciesielska A, et al. Safety and tolerability of MRI-guided infusion of AAV2-hAADC into the mid-brain of non-human primate. Mol Ther Methods Clin Dev. 2014:3. [PubMed: 26015942]

26. Richardson RM, Kells AP, Martin AJ, Larson PS, Starr PA, Piferi PG, et al. Novel platform for MRI-guided convection-enhanced delivery of therapeutics: preclinical validation in nonhuman primate brain. Stereotact Funct Neurosurg. 2011; 89(3):141–51. [PubMed: 21494065]

27. Insausti R, Amaral DG, Cowan WM. The entorhinal cortex of the monkey: II. Cortical afferents. J Comp Neurol. 1987; 264(3):356–95. [PubMed: 2445796]

28. Witter MP, Van Hoesen GW, Amaral DG. Topographical organization of the entorhinal projection to the dentate gyrus of the monkey. J Neurosci. 1989; 9(1):216–28. [PubMed: 2913203]

29. Witter MP, Amaral DG. Entorhinal cortex of the monkey: V. Projections to the dentate gyrus, hippocampus, and subicular complex. J Comp Neurol. 1991; 307(3):437–59. [PubMed: 1713237]

30. Amaral DG. Emerging principles of intrinsic hippocampal organization. Curr Opin Neurobiol. 1993; 3(2):225–9. [PubMed: 8390320]

31. Lavenex P, Amaral DG. Hippocampal-neocortical interaction: a hierarchy of associativity. Hippocampus. 2000; 10(4):420–30. [PubMed: 10985281]

32. Kirkby DL, Higgins GA. Characterization of perforant path lesions in rodent models of memory and attention. Eur J Neurosci. 1998; 10(3):823–38. [PubMed: 9753151]

33. Myhrer T, Naevdal GA. The temporal-hippocampal region and retention: the role of temporo-entorhinal connections in rats. Scand J Psychol. 1989; 30(1):72–80. [PubMed: 2740857]

34. Paxinos, G., Huang, XF., Toga, AW. The Rhesus Monkey Brain in Stereotaxic Coordinates. Academic Press; 1989.

35. Salegio EA, Kells AP, Richardson RM, Hadaczek P, Forsayeth J, Bringas J, et al. Magnetic resonance imaging-guided delivery of adeno-associated virus type 2 to the primate brain for the treatment of lysosomal storage disorders. Hum Gene Ther. 2010; 21(9):1093–103. [PubMed: 20408734]

36. Gimenez F, Krauze MT, Valles F, Hadaczek P, Bringas J, Sharma N, et al. Image-guided convection-enhanced delivery of GDNF protein into monkey putamen. Neuroimage. 2011; 54(Suppl 1):S189–95. [PubMed: 20080195]

37. Liu L, Drouet V, Wu JW, Witter MP, Small SA, Clelland C, et al. Trans-Synaptic Spread of Tau Pathology In Vivo. PLoS One. 2012; 7(2):E31302. [PubMed: 22312444]

38. Takeda S, Wegmann S, Cho H, DeVos SL, Commins C, Roe AD, et al. Neuronal uptake and propagation of a rare phosphorylated high-molecular-weight tau derived from Alzheimer's disease brain. Nat Commun. 2015; 6:8490. [PubMed: 26458742]

39. Olsson B, Lautner R, Andreasson U, Ohrfelt A, Portelius E, Bjerke M, et al. CSF and blood biomarkers for the diagnosis of Alzheimer's disease: a systematic review and meta-analysis. Lancet Neurol. 2016

40. Dubois B, Hampel H, Feldman HH, Scheltens P, Aisen P, Andrieu S, et al. Preclinical Alzheimer's disease: Definition, natural history, and diagnostic criteria. Alzheimers Dement. 2016; 12(3):292–323. [PubMed: 27012484]

41. Bevan AK, Duque S, Foust KD, Morales PR, Braun L, Schmelzer L, et al. Systemic gene delivery in large species for targeting spinal cord, brain, and peripheral tissues for pediatric disorders. Mol Ther. 2011; 19(11):1971–80. [PubMed: 21811247]

42. Arvanitakis Z, Tuszynski MH, Bakay R, Arends D, SP, Bartus R, et al. Interim data from a phase 1 clinical trial of AAV-NGF (CERE-110) gene delivery in Alzheimers disease. Abstr Amer Acad Neurol. 2007:05.071.

43. Rafii MS, Baumann TL, Bakay RA, Ostrove JM, Siffert J, Fleisher AS, et al. A phase1 study of stereotactic gene delivery of AAV2-NGF for Alzheimer's disease. Alzheimers Dement. 2014 Jan; 10(7):571–81. [PubMed: 24411134]

44. Salegio EA, Bringas J, Bankiewicz KS. MRI-Guided Delivery of Viral Vectors. Methods Mol Biol. 2016; 1382:217–30. [PubMed: 26611589]

45. Amaral DG, Insausti R, Cowan WM. The entorhinal cortex of the monkey: I. Cytoarchitectonic organization. J Comp Neurol. 1987; 264(3):326–55. [PubMed: 2445795]
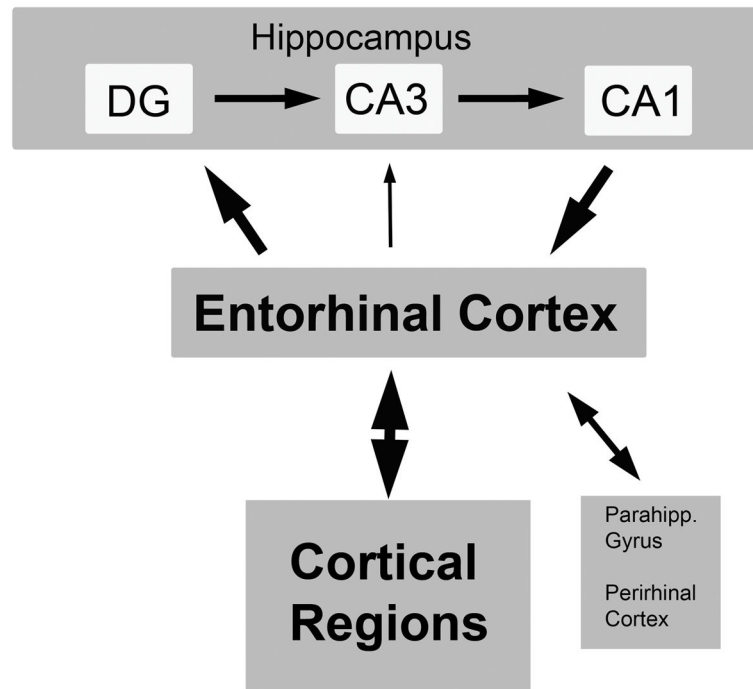
Figure 1. Schematic of entorhinal cortex and its major afferent and efferent connections with the hippocampus and the cerebral cortex

The major projections from the entorhinal cortex (layers II–III) are to the outer molecular layer of the dentate gyrus (DG) and CA3 region of the hippocampus. The CA1 region projects back to the deeper layers of the entorhinal cortex. The entorhinal cortex also directly projects to cortical regions that are sites of long-term memory storage[31].
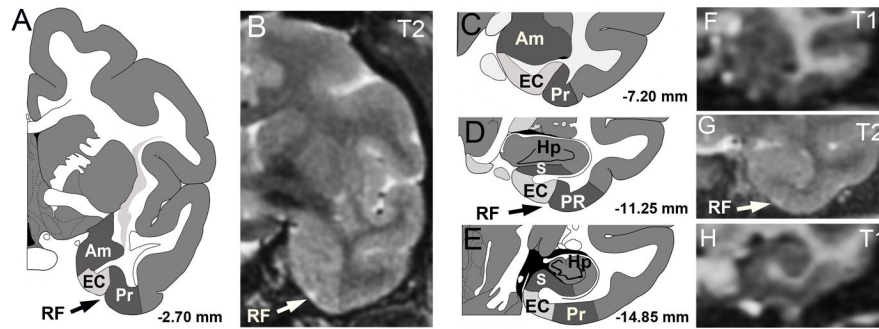
Figure 2. Location of entorhinal cortex (EC) in rhesus monkey with corresponding MR images
Schematic diagrams (adopted from Paxinos et al., 1989) of entorhinal cortex across four
coronal planes from −2.7 to −14.85 mm relative to bregma (**A, C–E**). The entorhinal cortex
is located on the ventral and medial surface of the temporal lobe, with local landmarks that
include the rhinal fissure (**RF**), perirhinal cortex (**PR**), amygdala (**Am**), subicular area (**S**),
and hippocampus (**Hp**). T1 and T2 MRI scans (**B, F–H**) with the visible landmark of the
rhinal fissure (**RF**) indicated on the T2 image (arrows in **A,B,D,G**).
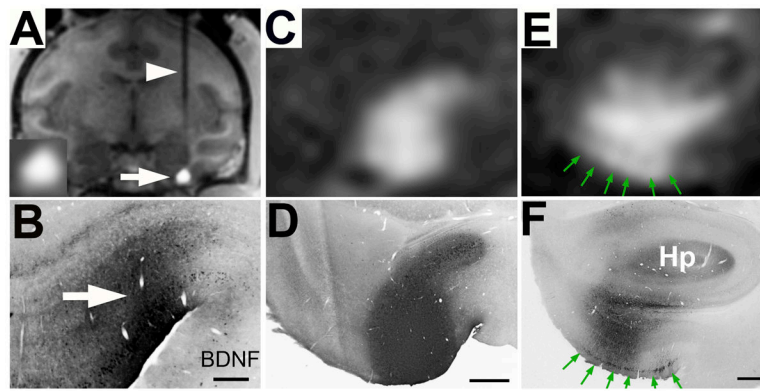
Figure 3. Real-time MRI scans of AAV2-BDNF delivery into the entorhinal cortex (entorhinal cortex) of non-human primate (A–C) result in accurately targeted BDNF delivery (D–F)
(**A**) An MR-compatible needle is present passing through the cortex and striatum (arrowhead) to reach the ventral and medial entorhinal cortex (arrow). The spread of gadoteridol in the infusion site is visible (arrow). Inset show gadoteridol signal at higher magnification. (**B**) A matching histological section from the same animal shows the spread of BDNF by immunolabeling in the same region predicted by MR imaging. (**C**) Pattern of gadolinium spread in a different subject within the entorhinal cortex on MR, and (**D**) the matching histological section. (**E**) Vector spread on MR in a 3rd subject, with gadolinium spread along cortical surface (green arrows), and (**F**) the matching BDNF immunolabeled section. Green arrows indicate a band of BDNF-containing, layer II entorhinal cells. Hp, hippocampus. Scale Bar, D = 0.5 mm, E–F = 1 mm.
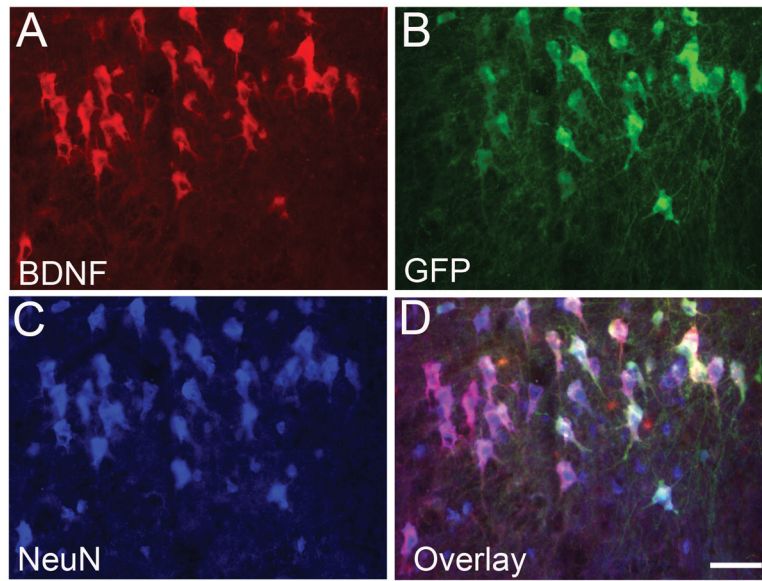
Figure 4. AAV2-BDNF and AAV2-GFP primarily transduce neurons
At the infusion site, (**A**) BDNF immunolabeling and (**B**) GFP immunolabeling are predominantly observed in neurons labeled with (**C**) NeuN. (**D**), overlay. On quantification, $88.2 \pm 3.8\%$ of GFP-expressing cells co-label for NeuN. Scale bar = 50 μm.
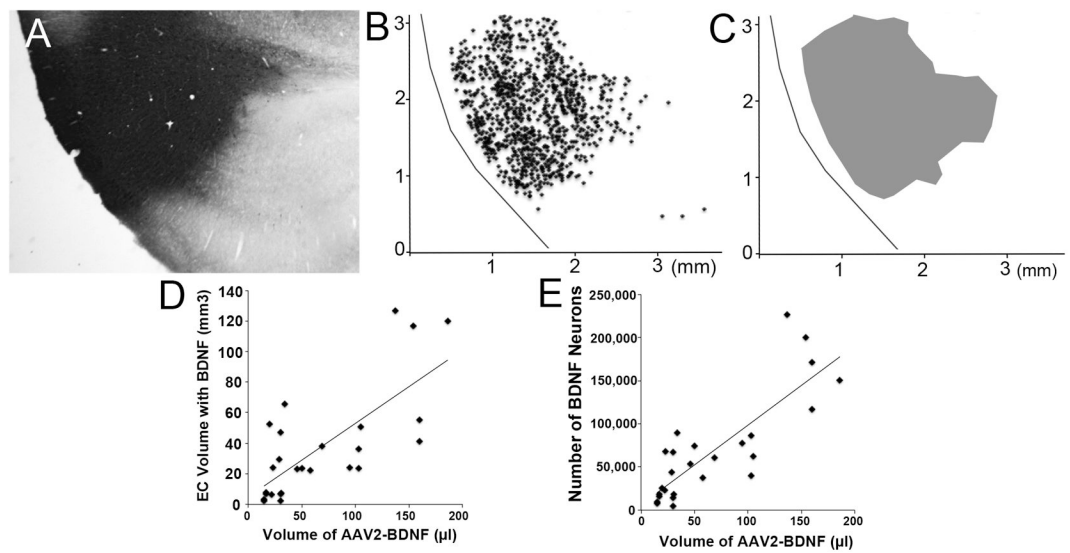
Figure 5. Distribution of BDNF-labeled neurons in entorhinal infusion sites
(**A**) BDNF immunolabeling in an AAV2-BDNF infusion site in the entorhinal cortex. (**B**) Map of individual cells immunolabeled for BDNF, and (**C**) zone of BDNF-containing cells used to quantify volume of vector distribution. (**D–E**) The volume of AAV2-BDNF vector infused significantly correlates with volume of tissue containing BDNF-labeled neurons (p<0.001) and with number of BDNF labeled neurons (p<0.001).
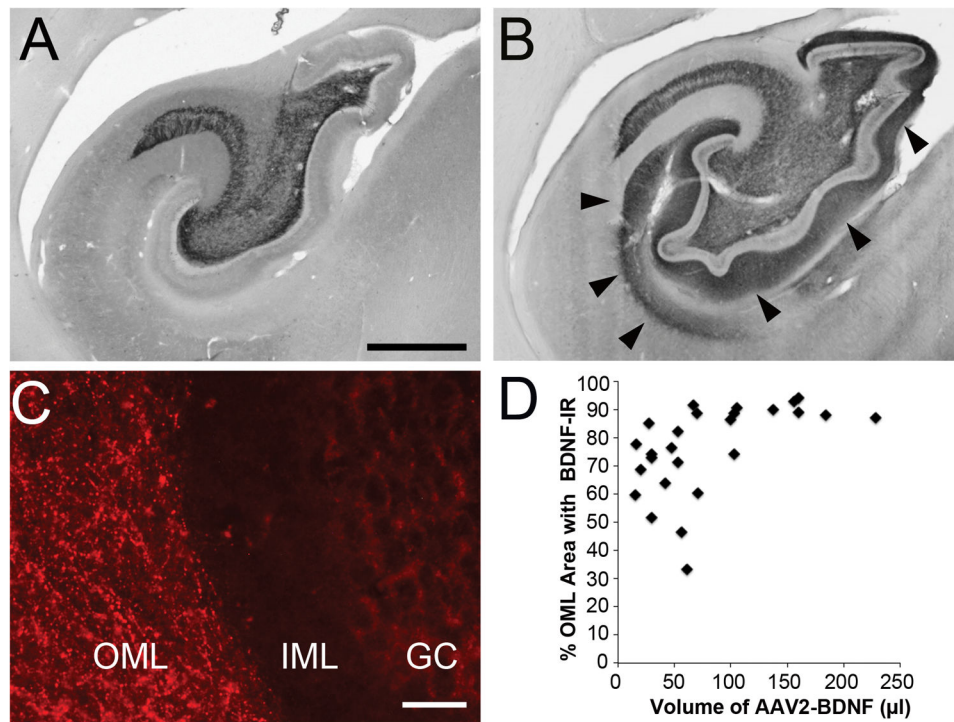
Figure 6. BDNF Spread to Hippocampus
(**A**) BDNF immunoreactivity in hippocampus of control subject shows endogenous expression of BDNF in the mossy fiber terminal fields of the CA3 lucidum and hilus region. (**B**) Following AAV2-BDNF infusion into entorhinal cortex, BDNF immunoreactivity is visible in the hippocampal outer molecular layers (arrowheads). (**C**) Fluorescent labeling illustrates BDNF immunoreactive fibers in the outer molecular layer (OML) and not in the inner molecular layer (IML) or granule cell layer (GC) of hippocampus. (**D**) Scatterplot showed that even smaller volumes of AAV2-BDNF infused into the entorhinal cortex can lead to a widespread (~70%) increase of BDNF expression in the OML of dentate gyrus. Scale bar A, B 1 mm; C, 200 μm.